High abundance of transcription regulators compacts the nucleoid in *Escherichia coli*

Cihan Yilmaz and Karin Schnetz*

Institute for Genetics, University of Cologne, Zülpicher Str. 47a, 50674 Cologne, Germany

*Corresponding author: schnetz@uni-koeln.de, +49-221-4703815

Keywords: transcription regulator, nucleoid structure, nucleoid compaction, nucleoid-associated protein

Running title: Nucleoid compaction by abundant DNA-binding proteins

Abstract

In enteric bacteria organization of the circular chromosomal DNA into a highly dynamic and toroidal shaped nucleoid involves various factors such as DNA supercoiling, nucleoid-associated proteins (NAPs), the structural maintenance of chromatin (SMC) complex, and macro-domain organizing proteins. Here we show that ectopic expression of transcription regulators at high levels leads to nucleoid compaction. This serendipitous result was obtained by fluorescence microscopy upon ectopic expression of the transcription regulator and phosphodiesterase PdeL of *Escherichia coli* of a strain expressing the mCherry-tagged HU-α subunit (HupA) for nucleoid staining. Nucleoid compaction by PdeL depends on DNA-binding, but not on its enzymatic phosphodiesterase activity. Nucleoid compaction was also observed upon high-level ectopic expression of the transcription regulators LacI, RutR, RcsB, LeuO and Cra, which range from single target gene regulators to global regulators. In case of LacI its high-level expression in presence of the gratuitous inducer IPTG also led to nucleoid compaction indicating that compaction is caused by unspecific DNA-binding. In all cases nucleoid compaction correlated with misplacement of the FtsZ ring and loss of MukB foci, a subunit of the SMC complex. Thus, high levels of several transcription regulators cause nucleoid compaction with consequences on transcription, replication, and cell division.

Importance

The bacterial nucleoid is a highly organized and dynamic structure for simultaneous, transcription, replication and segregation of the bacterial genome. Compaction of the nucleoid and disturbance of DNA segregation and cell division by artificially high levels of transcription regulators, as described here, reveals that an excess of DNA-binding protein disturbs nucleoid structuring. The results suggest that ectopic expression levels of DNA-binding proteins for genetic studies of their function but also for their purification should be carefully controlled and adjusted.

Introduction

Regulation of transcription in *Escherichia coli* involves a repertoire of approximately 300 transcription regulators of which more than 90% have been functionally validated (1-3). These transcription regulators include single target regulators such as LacI solely regulating the *lac* operon, local regulators with up to 50 target genes as for example RutR, a pyrimidine utilization repressor (4), and global regulators such as the catabolite activator repressor protein Cra and the pleiotropic regulator LeuO with more than 100 targets (5, 6). Nucleoid-associated proteins (NAPs) constitute a further group of DNA-binding proteins; they are abundant, relevant for organization of the genomic DNA as a nucleoid, and participate in the regulation of hundreds of targets genes (7).

PdeL, carrying a N-terminal FixJ/NarL/LuxR-type DNA-binding domain and a C-terminal EAL-type c-di-GMP-specific phosphodiesterase domain, is one of the validated transcriptional regulators with a small number of target loci including the *fliFGHIK* operon, *sslE*, and *pdeL* itself (8, 9). However, the physiological function of PdeL remains an open question, as a *pdeL* deletion mutant has no significant phenotype at least at the laboratory growth conditions (9). At these growth conditions expression of the *pdeL* gene and concomitantly PdeL protein levels are low, due to repression of *pdeL* by the abundant nucleoid-associated and global repressor protein H-NS (9, 10). However, moderately elevated PdeL levels using plasmids or up-regulated *pdeL* mutants disclosed its function as transcription regulator and as active c-di-GMP specific phosphodiesterase (8, 9). Furthermore, PdeL, as a dual function protein may represent a trigger enzyme whose role as transcription regulator is controlled by c-di-GMP via the phosphodiesterase domain (11).

Considering the dual functions of PdeL we used a fluorescent protein fusion, PdeL-mVenus, provided by a pBAD-derived plasmid to analyze its cellular localization. Serendipitously, we found that ectopic expression of PdeL causes nucleoid compaction even upon weak induction of the P_{ara} promoter directing expression of *pdeL-mVenus*. Weak induction nonetheless led to high levels of PdeL, which is a very stable protein. Further, other transcription regulators (LacI, RutR, RcsB, LeuO, and Cra) all cause compaction of the nucleoid as well, when expressed and synthesized at similarly high levels. The data indicate that the mere occupation of the genomic DNA by an abundant DNA-binding protein can have severe effects on nucleoid structuring.

Results

PdeL is nucleoid-associated and causes nucleoid compaction

Here we addressed whether the dual function protein PdeL is predominantly nucleoid-associated or localized otherwise. To this end, PdeL-mVenus fusions were provided by plasmids under control of the P_{ara} promoter, and the cellular localization was analyzed by fluorescence microscopy in *E. coli hupA-mCherry* Δ*pdeL* strain U159 (Fig. 1A, Tables 1 and 2). In this strain gradual induction of P_{ara} by arabinose is applicable due to modification of the arabinose regulon, as described (12, 13), while HupA-fluorescent protein fusions are well-established markers for nucleoid imaging (14, 15). Cellular localization of PdeL-mVenus and of $PdeL_{HTH5M}$-mVenus, a mutant defective in DNA-binding as a control, was analyzed (9). Note that chromosomal encoded PdeL-mVenus is not detectable by fluorescence microscopy due to low expression of the *pdeL* gene (9).

First, we determined the L-arabinose concentration needed for inducing the synthesis of equal amounts of PdeL and the DNA-binding defective control $PdeL_{HTH5M}$ by using 3xFLAG alleles carried on the same plasmidic expression system as used for fluorescence microscopy (Fig. S1). PdeL-3xFLAG gene expression was induced with 2µM L-arabinose, while expression of $PdeL_{HTH5M}$-3xFLAG was induced by addition of increasing concentrations of L-arabinose. The amount of PdeL-3xFLAG (induced by addition of 2 µM L-arabinose) and $PdeL_{HTH5M}$-3xFLAG (induced with 20 µM L-arabinose) were similar (Fig. S1). The low concentration of L-arabinose that is required for synthesis of significant amounts of PdeL indicates that PdeL synthesis is efficient and that the PdeL protein is stable. Determination of the protein stability of PdeL and $PdeL_{HTH5M}$ showed that PdeL-3xFLAG was stable for 160 minutes after inhibition of translation by 100 µg/ml chloramphenicol (Fig. S1). In contrast, the $PdeL_{HTH5M}$-3xFLAG steady state level was lower and its level decreased approximately 2-fold in the 160 minutes after inhibition of translation, which suggests that $PdeL_{HTH5M}$ is less stable than PdeL (Fig. S1). Note that protein stability was determined without induction to keep PdeL-levels sufficiently low for quantification (Fig. S1). The result of the protein stability assay is in accordance with the different concentrations of L-arabinose that are required for similar steady state protein levels of PdeL-3xFLAG and $PdeL_{HTH5M}$-3xFLAG.

For fluorescence microscopy plasmidic P_{ara}-directed expression of *pdeL-Venus* and *pdeL*$_{HTH5M}$-*mVenus* was induced by L-arabinose after one hour of growth (t = 1h), and samples were harvested after one and two additional hours of growth (at t=2h and t=3h) later (Fig. 1). PdeL-mVenus fluorescence was apparent after one hour of induction and localized to the whole nucleoid (Fig. 1B and Fig. S2). In addition, nucleoid-association was accompanied by nucleoid compaction, formation of nucleoid free areas near the cell poles, and an enlargement of the bacteria. In contrast, PdeL$_{HTH5M}$-mVenus was located diffusely in the cell, and after two hours of induction, aggregates of PdeL$_{HTH5M}$-mVenus near the cell pole became apparent. Taken together, the data suggest that the transcription regulator PdeL is nucleoid-associated and they indicate that DNA-binding by high PdeL levels cause nucleoid compaction.

PdeL and RcsB compact the nucleoid and affect localization of MukB-mNeonGreen

PdeL-mVenus leads to nucleoid compaction close to midcell. Since the nucleoid structure is changed, we tested localization of MukB, a subunit of the structural maintenance of chromosome (SMC) complex and a marker for *oriC* localization, using chromosomally encoded MukB-mNeonGreen (MukB-mNG) (16-19). In addition, FtsZ-mNG was used as a marker for septum formation (for results see below). In this experimental approach, transformants expressing non-tagged PdeL, the DNA-binding defective, PdeL$_{HTH5M}$, and an enzymatically inactive PdeL$_{EVL\text{-}AAA}$ were studied (Fig. 2A). PdeL$_{EVL\text{-}AAA}$ is enzymatically inactive due to mutation of the conserved c-di-GMP-specific EVL motif to three alanine residues. In addition to PdeL, high level expression of the two-component response regulator RcsB was included, which like PdeL carries a FixJ/NarL/LuxR-type DNA-binding domain, to analyze whether nucleoid compaction by high protein levels is PdeL-specific.

First, synthesis of RcsB levels that are similar to the levels of PdeL were established using plasmids carrying 3xFLAG-tagged *rcsB* alleles under P_{ara} control (Fig. S3). In these plasmids the efficiency of translation of *rcsB-3xFLAG* was varied. RcsB-3xFLAG levels were lowest with its native ribosomal binding site (RBS), higher when *rcsB* was fused to *pdeL's* RBS, and similarly high as PdeL levels when using the phage *T7 gene10* RBS and 50 µM of L-arabinose for induction (Fig. S3).

Next, fluorescence microscopy was performed using transformants of *hupA-mCherry mukB-mNG* Δ*pdeL* strain U477 with plasmids coding for PdeL, PdeL$_{HTH5M}$, PdeL$_{EVL\text{-}AAA}$, and RcsB,

respectively. These transformants synthesized approximately equal amounts of PdeL, $PdeL_{HTH5M}$, $PdeL_{EVL\text{-}AAA}$ and RcsB upon induction by L-arabinose, as shown by SDS-PAGE (Fig. 2A). Induction of high levels of PdeL, $PdeL_{EVL\text{-}AAA}$, and RcsB synthesis caused nucleoid compaction to midcell and a moderate increase of the cell length (Fig. 2B). Furthermore, one or two MukB-mNG foci close to *oriC* were detectable without induction and in the control (Fig. 2B and Fig. S4), as previously shown for fluorescent protein MukB fusions (17). MukB-mNG foci disappeared upon induction of PdeL, $PdeL_{EVL\text{-}AAA}$, and RcsB expression, but were not changed in case of the DNA-binding deficient $PdeL_{HTH5M}$ (Fig. 2B). The disappearance of MukB-mNG foci was not caused by a change in the MukB protein levels, which remained constant (Fig. S5). Taken together, high protein levels of PdeL and RcsB, but not of the DNA-binding defective $PdeL_{HTH5M}$ mutant led to nucleoid compaction and loss of MukB-mNG foci.

High levels of PdeL and RcsB proteins lead to misplacement of the FtsZ ring

As a second marker we tested whether localization of cell division protein FtsZ is affected by synthesis of high levels of PdeL and RcsB. For visualization of the Z-ring in *ftsZ*$^+$ background, FtsZ-mNG was provided by a low-copy plasmid carrying a P_{lacUV5} *ftsZ-mNG* cassette, as described (20). The low activity of the non-induced P_{lacUV5} promoter was sufficient for production of detectable amounts of FtsZ-mNG. Fluorescence microscopy was performed with double transformants of *hupA-mCherry* Δ*pdeL* strain U159 with the *ftsZ-mNG* plasmid and compatible *pdeL* or *rcsB* carrying plasmids (Fig. 3). Depending on the progression of the cell cycle, FtsZ-mNG was detectable at midcell forming the Z-ring, in case of the control and the $PdeL_{HTH5M}$ DNA-binding mutant (Fig. 3 and Fig. S6). Localization of FtsZ-mNG was different when PdeL and when RcsB were expressed at high levels. In these cases, the FtsZ was displaced from mid-cell towards the quarter positions which are devoid of the nucleoid (Fig. 3 and Fig. S6). Taken together, the FtsZ ring is misplaced by high levels of PdeL, $PdeL_{EVL\text{-}AAA}$, and RcsB, but not by the DNA-binding defective $PdeL_{HTH5M}$ (Fig. 3 and Fig. S6).

High levels of the transcription regulators LacI, RutR, LeuO, and Cra also cause nucleoid compaction

Since high levels of both PdeL and RcsB affect the nucleoid structure and localization of MukB and FtsZ, we tested additional DNA-binding proteins. This included the single target transcription regulator LacI, the local regulator RutR, and the global regulators LeuO and Cra

(6). Plasmidic P_{ara} directed expression of these transcription regulators was adjusted to obtain approximately equal amounts of each protein, as validated by SDS-PAGE (Fig. S7). Fluorescence microscopy demonstrated that high levels of all transcription regulators, LacI, RutR, LeuO, and Cra, caused nucleoid compaction as well (Fig. 4 and Fig. S8). In addition, we also analyzed whether LacI in presence of IPTG causes the same phenotype. Specific DNA-binding of LacI is inhibited by IPTG (21). Non-specific DNA-binding of high levels of LacI-IPTG was sufficient to cause compaction of the nucleoid (Fig. 5 and S9). In all cases the number of MukB-mNG foci was significantly lower (Figs. 4, 5, S8, and S10). Taken together, all tested transcription regulators LacI, RutR, LeuO, and Cra caused nucleoid compaction and a decrease of MukB-mNG foci similar to PdeL and RcsB.

For RutR, LeuO and Cra we also tested FtsZ localization using low-copy plasmid carrying *ftsZ-mNG* under control of the LacI-regulated *lacUV5* promoter (Fig. 6 and S10). In this experiment LacI could not be included, since high levels of LacI led to complete inhibition of *ftsZ-mNG* expression. Fluorescence microscopy of the transformants expressing high levels of RutR, LeuO and Cra, respectively, caused misplacement of the FtsZ similarly as PdeL and RcsB (Fig. 6).

Lastly, the amount of PdeL that is synthesized upon induction of P_{ara} by 2 µM L-arabinose was estimated using purified PdeL-His_6 as a reference (Fig. S11). After one hour of induction, approximately 40,000 PdeL monomers and after two hours of induction approximately 150,000 monomers of PdeL are present per cell, which corresponds to one PdeL dimer per 250 bp after one hour and four PdeL dimers per 250 bp after two hours of induction (assuming that a single non-replicating nucleoid is present).

Discussion

Here we have shown that high levels of the transcription regulators PdeL, RcsB, LacI, RutR, Cra, and LeuO lead to nucleoid compaction in *E. coli*. These transcription regulators include single target and local regulators with only one or few specific DNA-binding sites and global regulators with hundreds of DNA-binding sites in the genome (6). Our data suggest that nucleoid compaction is caused by non-specific occupancy of the genomic DNA. Comparable observations of nucleoid compaction have been described recently for the phage T4 protein MotB and for the bacterial DNA-binding toxin SymE (22, 23).

The dual function protein PdeL, a transcription regulator and c-di-GMP specific phosphodiesterase, is nucleoid-associated. Further, ectopic expression of *pdeL* directed by weak induction of P_{ara} resulted in a high cellular protein level, apparently because PdeL is a protein of high stability. The high level of PdeL caused nucleoid compaction. Likewise, the two-component response regulator RcsB, which carries a FixJ/NarL/LuxR-type DNA-binding domain like PdeL, caused nucleoid compaction, when expressed at similarly high levels as PdeL. Other transcription regulators led to nucleoid compaction as well, and this is independent of the number of specific DNA-binding sites, as shown with the single target regulator LacI, the local regulator RutR, and the global regulators Cra and LeuO (5, 6). In case of LacI nucleoid compaction is independent of specific DNA-binding as shown using the gratuitous inducer IPTG.

The high level of PdeL with approximately 40,000 molecules per cell one hour after induction corresponds to one dimer per 250 bp, while the approximately 150,000 molecules present after two hours of ectopic synthesis would theoretically allow complete coverage of the genome. The cellular levels of the other transcription regulators tested in this study are comparable. Occupancy of the whole genome by a DNA-binding could hinder DNA replication and/or transcription. In case of the toxin SymE it has been shown that toxicity of *symE* overexpression is presumably based on nucleoid condensation and inhibition of DNA as well as RNA synthesis (23). Further, these authors have shown that nucleoid compaction caused by synthesis of SymE at high levels is similar to nucleoid compaction caused by overexpression of H-NS (23, 24). Such a mechanism of genome silencing is possibly utilized by phage T4, which encodes the protein MotB that shortly after infection is synthesized at very high levels corresponding to 40,000 monomers per cell (22). In case of phage T4 MotB, fluorescence

209 imaging using a MotB-GFP fusion demonstrated nucleoid compaction (22) similar to the data
210 shown in this work. Interestingly, MotB has dramatic effects on the transcriptome leading to
211 a relative increase of 1/8 of all transcripts in relation to the whole transcriptome, and of these
212 1/8 of the transcriptome ~70% correspond to H-NS repressed genes (22, 25). Thus, phage T4
213 apparently employs the abundance of MotB to re-program the host transcriptome (22).
214 Remarkably, nucleoid-associated proteins (NAPs) such as H-NS, HU, IHF, and FIS and others
215 are abundant (26), but at their natural level they do not cause nucleoid compaction. H-NS,
216 present at approximately 20,000 molecules per cell binds to the minor groove of AT-rich DNA
217 and forms linear and bridged filaments. HU and IHF are likewise abundant and DNA-bending
218 proteins that presumably contribute to nucleoid structuring and formation of specific
219 regulatory nucleoprotein complexes. FIS is expressed at very high levels with 50,000
220 molecules per cell during the early exponential growth phase only; it is a DNA-bending protein
221 and organizer of plectonemic structures (7, 27). The cellular levels of the abundant NAPs is
222 apparently well adjusted to their function.

223 Our data suggest that compaction of the nucleoid by the transcription regulators displaces Z-
224 rings from mid-cell towards the cell poles. Exclusion of the Z-ring from midcell can be an
225 indirect effect mediated by the nucleoid occlusion system and SlmA protein (28). Similarly,
226 the loss of detectable MukB-mNeonGreen foci near the origin of replication can be an indirect
227 consequence of nucleoid compaction, as it is possible that DNA replication is put on hold by
228 excessive occupancy of the genome by overexpressed transcription regulators. In accordance
229 with an indirect effect, the change in positioning of MukB and the FtsZ is observed later than
230 nucleoid compaction.

231 The serendipitous finding reported here emphasizes the importance of using native protein
232 levels in functional analysis of transcription regulators. Another aspect to be considered when
233 using ectopic expression is that the level of a transcription regulator and the number of its
234 specific DNA-binding sites in the genome is balanced (29). Ectopic expression can be required
235 for a functional analysis, as for example when conditions leading to expression of the gene
236 encoding a transcription regulator and an inducer are not known. In case of transcription
237 regulators that are stable, such as PdeL, ectopic expression even for a short time and with a
238 low inducer concentration may yield far too high protein levels. Thus, if an ectopic expression

239 system is used, the rate and duration of synthesis as well as the protein stability and cellular
240 level should be controlled carefully.

Material and Methods

Bacterial strains media and plasmids

E. coli K12 strains and their construction are described in Table 1. Strains were constructed by transduction using phage T4*GT7* or P1 *vir*, and by Lambda-Red-mediated recombineering, respectively (30-33). Plasmids are listed in Table 2 and oligonucleotides used for construction of strains and plasmids are listed in supplementary Table S1. Bacteria were cultured in in LB medium (10 g/l tryptone, 5 g/l yeast extract, and 5 g/l NaCl), tryptone medium (10 g/l tryptone, 5 g/l NaCl), SOB medium (20 g/l tryptone, 5 g/l yeast extract, 0.5 g/l NaCl, 2.5 mM KCl, 10 mM $MgCl_2$, pH7.0), or SOC (SOB with 0.4 % glucose). For plates, 15 g/l agar were added. Antibiotics were added to a final concentration of 50 µg/ml ampicillin, 15 µg/ml chloramphenicol, and 15 µg/ml kanamycin, as required; IPTG and L-arabinose, respectively, were added as described in the figures.

Fluorescence microscopy

For fluorescence microscopy transformants of *E. coli* strain U159 (U65 *hupA-mCherry*$_{FRT}$ Δ*pdeL*$_{FRT}$) and its derivatives were inoculated to OD_{600} of 0.08 in tryptone medium supplemented with appropriate antibiotics and grown at 37°C whilst shaking. Plasmid P_{ara} directed expression of the transcription regulators was induced after one hour of growth by adding L-arabinose at the concentration stated in the figures. Bacteria were harvested just before induction (t = 1h), and one and two hours after induction (at t = 2h and t = 3h) by pelleting 500 µl of the culture by centrifugation at 5900 r.c.f. for 1 minute. The bacterial pellets were resuspended in 150 µl of fresh tryptone medium, and 4 µl of these suspensions were spotted onto 1% agarose pads for microscopy. Image acquisition was performed using Zeiss Axio Imager.M2 microscope with an EC Plan-Neofluar 100x/1.30 Oil Ph3 M27 objective. Images were captured and processed using ZEN 2012 software (Carl Zeiss Microscopy GmbH, Germany). Excitation times were 500 ms for PdeL-mVenus fusions, MukB-mNG, FtsZ-mNG and HupA-mCherry. Contrast settings were 1-16384 for phase contrast, 200-2000 for HupA-mCherry, 1-16384 for PdeL-mVenus, 180-300 for MukB-mNG and 180-1000 for FtsZ-mNG, unless otherwise stated in the figures.

PdeL protein stability analyses

For determining the protein stability of PdeL and its variants, transformants of *E. coli* strain U121 (U65 Δ*pdeL*$_{FRT}$) with plasmids pKECY81 (*P*$_{ara}$ *pdeL-3xFLAG*) and pKECY91 (*P*$_{ara}$ *pdeL*$_{HTH5M}$-*3xFLAG*) were inoculated to an OD_{600} of 0.08 in tryptone medium supplemented with ampicillin. The transformants were grown for 2 hours at 37°C without induction of *P*$_{ara}$ to preserve a low protein level for quantification by western blotting. Translation was blocked by adding chloramphenicol to a final concentration of 100 µg/ml. Samples of 2 ml volume were taken just prior and at several time points after inhibition of translation. Bacteria were pelleted by centrifugation and re-suspended in Laemmli buffer for detection of epitope-tagged protein by Western blotting (34)}.

Protein detection by western blotting and coomassie staining

SDS-PAGE, Coomassie staining, and Western blots were performed as described (34). Unless otherwise described, bacteria equivalent to an OD_{600} of 0.08 were loaded per lane. Equal loading was validated by 2,2,2-trichloroethane (TCE) staining of total protein (35). Epitope-tagged 3xFLAG proteins were detected using primary antibody anti-FLAG M2 from mouse (diluted 1:4,000, catalogue number F3165; Sigma Aldrich, Germany) and Alexa Fluor 680 fluorescent dye-labeled secondary anti-mouse antibody from goat (diluted 1:10,000, catalogue number A21057; Thermo Scientific, Germany). Quantification of protein bands was performed with Odyssey V3.0 software for Western blots and with ImageLab (BioRad, Germany) for Coomassie stained gels.

References

1. Pérez-Rueda E, Collado-Vides J. 2000. The repertoire of DNA-binding transcriptional regulators in Escherichia coli K-12. Nucleic Acids Res 28:1838-1847.
2. Santos-Zavaleta A, Salgado H, Gama-Castro S, Sánchez-Pérez M, Gómez-Romero L, Ledezma-Tejeida D, García-Sotelo JS, Alquicira-Hernández K, Muñiz-Rascado LJ, Peña-Loredo P, Ishida-Gutiérrez C, Velázquez-Ramírez DA, Del Moral-Chávez V, Bonavides-Martínez C, Méndez-Cruz C-F, Galagan J, Collado-Vides J. 2018. RegulonDB v 10.5: tackling challenges to unify classic and high throughput knowledge of gene regulation in E. coli K-12. Nucleic Acids Res 47:D212-D220.
3. Gao Y, Lim HG, Verkler H, Szubin R, Quach D, Rodionova I, Chen K, Yurkovich JT, Cho B-K, Palsson Bernhard O. 2021. Unraveling the functions of uncharacterized transcription factors in Escherichia coli using ChIP-exo. Nucleic Acids Res 49:9696-9710.
4. Shimada T, Ishihama A, Busby SJW, Grainger DC. 2008. The Escherichia coli RutR transcription factor binds at targets within genes as well as intergenic regions. Nucleic Acids Res 36:3950-3955.
5. Ishihama A, Shimada T, Yamazaki Y. 2016. Transcription profile of *Escherichia coli*: genomic SELEX search for regulatory targets of transcription factors. Nucleic Acids Res 44:2058-2074.
6. Shimada T, Ogasawara H, Ishihama A. 2018. Single-target regulators form a minor group of transcription factors in Escherichia coli K-12. Nucleic Acids Res 46:3921-3936.
7. Dame RT, Rashid F-ZM, Grainger DC. 2020. Chromosome organization in bacteria: mechanistic insights into genome structure and function. Nat Rev Genet 21:227-242.
8. Reinders A, Hee C-S, Ozaki S, Mazur A, Boehm A, Schirmer T, Jenal U. 2016. Expression and genetic activation of cyclic di-GMP-specific phosphodiesterases in *Escherichia coli*. J Bacteriol 198:448-462.
9. Yilmaz C, Rangarajan AA, Schnetz K. 2020. The transcription regulator and c-di-GMP phosphodiesterase PdeL represses motility in *Escherichia coli*. J Bacteriol 203:JB.00427-20.
10. Rangarajan AA, Schnetz K. 2018. Interference of transcription across H-NS binding sites and repression by H-NS. Mol Microbiol 108:226-239.
11. Hengge R. 2016. Trigger phosphodiesterases as a novel class of c-di-GMP effector proteins. Philos Trans R Soc Lond B Biol Sci 371:20150498.
12. Breddermann H, Schnetz K. 2016. Correlation of antagonistic regulation of *leuO* transcription with the cellular levels of BglJ-RcsB and LeuO in *Escherichia coli*. Front Cell Infect Microbiol 6:106.
13. Khlebnikov A, Risa Ø, Skaug T, Carrier TA, Keasling JD. 2000. Regulatable arabinose-inducible gene expression system with consistent control in all cells of a culture. J Bacteriol 182:7029-7034.
14. Wery M, Woldringh CL, Rouviere-Yaniv J. 2001. HU-GFP and DAPI co-localize on the Escherichia coli nucleoid. Biochimie 83:193-200.
15. Marceau AH, Bahng S, Massoni SC, George NP, Sandler SJ, Marians KJ, Keck JL. 2011. Structure of the SSB–DNA polymerase III interface and its role in DNA replication. EMBO J 30:4236-4247.

16. Niki H, Jaff, A, Imamura R, Ogura T, Hiraga S. 1991. The new gene *mukB* codes for a 177 kd protein with coiled-coil domains involved in chromosome partitioning of E.coli EMBO J 10:183-193.
17. Danilova O, Reyes-Lamothe R, Pinskaya M, Sherratt D, Possoz C. 2007. MukB colocalizes with the oriC region and is required for organization of the two Escherichia coli chromosome arms into separate cell halves. Mol Microbiol 65:1485-1492.
18. Badrinarayanan A, Reyes-Lamothe R, Uphoff S, Leake MC, Sherratt DJ. 2012. In Vivo Architecture and Action of Bacterial Structural Maintenance of Chromosome Proteins. Science 338:528-531.
19. Mäkelä J, Sherratt DJ. 2020. Organization of the Escherichia coli Chromosome by a MukBEF Axial Core. Mol Cell 78:250-260.e5.
20. Bernhardt TG, de Boer PAJ. 2005. SlmA, a Nucleoid-Associated, FtsZ Binding Protein Required for Blocking Septal Ring Assembly over Chromosomes in E. coli. Mol Cell 18:555-564.
21. Lewis M. 2005. The lac repressor. Comptes Rendus Biologies 328:521-548.
22. Son B, Patterson-West J, Arroyo-Mendoza M, Ramachandran R, Iben James R, Zhu J, Rao V, Dimitriadis Emilios K, Hinton Deborah M. 2021. A phage-encoded nucleoid associated protein compacts both host and phage DNA and derepresses H-NS silencing. Nucleic Acids Res 49:9229-9245.
23. Thompson MK, Nocedal I, Culviner PH, Zhang T, Gozzi KR, Laub MT. 2021. Escherichia coli SymE is a DNA-binding protein that can condense the nucleoid. Mol Microbiol https://doi.org/10.1111/MMI.14877.
24. Spurio R, D□rrenberger M, Falconi M, La Teana A, Pon CL, Gualerzi CO. 1992. Lethal overproduction of the Escherichia coli nucleoid protein H-NS: Ultramicroscopic and molecular autopsy. MolGenGenet 231:201-211.
25. Patterson-West J, Tai C-H, Son B, Hsieh M-L, Iben JR, Hinton DM. 2021. Overexpression of the Bacteriophage T4 motB Gene Alters H-NS Dependent Repression of Specific Host DNA. Viruses 13:84.
26. Talukder AA, Iwata A, Nishimura A, Ueda S, Ishihama A. 1999. Growth Phase-Dependent Variation in Protein Composition of the Escherichia coli Nucleoid. J Bacteriol 181:6361-6370.
27. Lioy VS, Junier I, Boccard F. 2021. Multiscale Dynamic Structuring of Bacterial Chromosomes. Annu Rev Microbiol 75:541-561.
28. Wu LJ, Errington J. 2012. Nucleoid occlusion and bacterial cell division. Nat Rev Microbiol 10:8-12.
29. Gao R, Helfant LJ, Wu T, Li Z, Brokaw SE, Stock Ann M. 2021. A balancing act in transcription regulation by response regulators: titration of transcription factor activity by decoy DNA binding sites. Nucleic Acids Res 49:11537-11549.
30. Wilson GG, Young KYK, Edlin GJ, Konigsberg W. 1979. High-frequency generalised transduction by bacteriophage T4. Nature 280:80-82.
31. Miller JH. 1992. A short course in bacterial genetics. A laboratory manual and handbook for *Escherichia coli* and related bacteria. Cold Spring Harbor Laboratory Press, Plainview, New York, USA.
32. Datsenko KA, Wanner BL. 2000. One-step inactivation of chromosomal genes in *Escherichia coli* K-12 using PCR products. Proc Natl Acad Sci USA 97:6640-6645.
33. Uzzau S, Figueroa-Bossi N, Rubino S, Bossi L. 2001. Epitope tagging of chromosomal genes in *Salmonella*. Proc Natl Acad Sci USA 98:15264-15269.

34. Sambrook J, Russell D. 2001. Molecular cloning: a laboratory manual, vol 3. Cold Spring Harbor Laboratory Press, Cold Spring Harbor, NY.
35. Ladner CL, Yang J, Turner RJ, Edwards RA. 2004. Visible fluorescent detection of proteins in polyacrylamide gels without staining. Anal Biochem 326:13-20.
36. Pannen D, Fabisch M, Gausling L, Schnetz K. 2016. Interaction of the RcsB response regulator with auxiliary transcription regulators in *Escherichia coli*. J Biol Chem 291:2357-2370.
37. Guzman LM, Belin D, Carson MJ, Beckwith J. 1995. Tight regulation, modulation, and high-level expression by vectors containing the arabinose P_{BAD} promoter. J Bacteriol 177:4121-4130.
38. Cherepanov PP, Wackernagel W. 1995. Gene disruption in Escherichia coli: TcR and KmR cassettes with the option of Flp-catalyzed excision of the antibiotic-resistance determinant. Gene 158:9-14.
39. Venkatesh GR, Kembou Koungni FC, Paukner A, Stratmann T, Blissenbach B, Schnetz K. 2010. BglJ-RcsB heterodimers relieve repression of the *Escherichia coli bgl* operon by H-NS. J Bacteriol 192:6456-6464.
40. Fragel SM, Montada A, Heermann R, Baumann U, Schacherl M, Schnetz K. 2019. Characterization of the pleiotropic LysR-type transcription regulator LeuO of Escherichia coli. Nucleic Acids Res 47:7363-7379.

Tables

Table 1: E. coli K12 strains

Strain	Genotype	Reference/Construction[a]
T1241	BW30270 ilvG$^+$ flhDC(IS1); motile	(36)
Donor strains for transduction		
T2817	T1241 *mukB-3xFLAG*$_{kan}$	T1241/pKD46 x OB68/OB69 (pSUB11)
T2818	T1241 *mukB-mNG*$_{cm}$	T1241/pKD46 x OB66/OB67 (pKECY38)
U98	T1241 Δ*pdeL*$_{cm}$	(9)
U65 and derivatives		
U65	T1241 Δ(*araC-BAD*) Δ*lac*(*I-ZYA*)$_{FRT}$ P$_{cp8}$ *araE* Δ*araFGH flhDC*$^+$	(12)
U119	U65 Δ*pdeL*$_{cm}$	U65 x T4*GT7* (U98)
U121	U65 Δ*pdeL*$_{FRT}$	U119 x pCP20
U148	U65 Δ*pdeL*$_{FRT}$ *hupA-mCherry*$_{kan}$	U121/pKD46 x OA484/OA485 (pKECY15)
U159	U65 Δ*pdeL*$_{FRT}$ *hupA-mCherry*$_{FRT}$	U148 x pCP20
U471	U65 Δ*pdeL*$_{FRT}$ *hupA-mCherry*$_{FRT}$ *mukB-mNG*$_{cm}$	U159 x P1*vir*(T2818)
U477	U65 Δ*pdeL*$_{FRT}$ *hupA-mCherry*$_{FRT}$ *mukB-mNG*$_{FRT}$	U471 x pCP20
U466	U65 *mukB-3xFLAG*$_{kan}$	U65 x P1*vir*(T2817)
U473	U65 *mukB-3xFLAG*$_{FRT}$	U466 x pCP20
U467	U65 Δ*pdeL*$_{FRT}$ *mukB-3xFLAG*$_{kan}$	U121 x P1*vir*(T2817)
U474	U65 Δ*pdeL*$_{FRT}$ *mukB-3xFLAG*$_{FRT}$	U467 x pCP20

[a] Strains were constructed by transduction, which is stated as "x phage[donor strain]"; λ Red recombineering, stated as "x PCR primer pair (template)," followed by Flp recombinase-catalyzed deletion of the resistance marker, "x pCP20".

Table 2	**Plasmids**	
Plasmid	**Features** [a]	**Construction/Reference** [b]
pBAD30	*araC* P_{ara} MCS in p15A-ori; Amp^R	(37)
pCP20	cI_{857} P_R flp in pSC101-rep^{ts} Amp^R	(38)
pKD3	FRT-*cmR*-FRT in oriRγ Amp^R	(32)
pKD4	FRT-*kanR*-FRT in oriRγ Amp^R	(32)
pKD46	*araC* P_{ara} γ-β-exo in pSC101-rep^{ts} Amp^R	(32)
pSUB11	3xFLAG in pKD4	(33)
pKESK22	*lacI*^{q} P_{tac} MCS in p15A-ori; Kan^r	(39)
pKETS24	*lacI* P_{lacUV5} in pSC-ori Cm^R	(40)
pKESL165	*lacI*^{q} P_{tac} *mVenus* in pKESK22	(9)
pKESL209	*lacI*^{q} P_{tac} *pdeL*$_{HTH5M}$-*mVenus* in pKESK22	(9)
pKEHB12	3xFLAG in pBAD30	*3xFLAG* (annealed oligos T687/T906) in pBAD30
pKEHB23	*araC* P_{ara} *mVenus* in pBAD30	*mVenus* (pKESL165 EcoRI/XbaI) in pBAD30
pKECY1	*araC* P_{ara} *pdeL-mVenus* in pBAD30	*pdeL* (T925/T952) in pKEHB23
pKECY11	*araC* P_{ara} *pdeL*$_{HTH5M}$-*mVenus* in pBAD30	*pdeL*$_{HTH5M}$ (T925/T952 from pKESL209) in pKEHB23
pKECY15	*mCherry* in pKD4	*mCherry* (PCR OA480/OA481) in pKD4
pKECY26	*mNeonGreen* in pSC-ori Cm^R	(9)
pKECY38	*mNeonGreen* in pKD3	*mNeonGreen* (SalI, BamHI from pKECY26)
pKECY43	*ftsZ-mNeonGreen* in in pSC-ori Cm^R	*ftsZ* (PCR OA807/OA808) in pKECY26 (XbaI, NdeI)
pKECY44	*araC* P_{ara} *pdeL* in pBAD30	(9)
pKECY52	*araC* P_{ara} *pdeL*$_{HTH5M}$ in pBAD30	(9)
pKECY53	*araC* P_{ara} *pdeL*$_{EVL-AAA}$ in pBAD30	(9)
pKECY81	*araC* P_{ara} *pdeL-3xFLAG* in pBAD30	*pdeL* (T925/OA116) in pKEHB12
pKECY90	*lacI* P_{lacUV5} *ftsZ-mNeonGreen* in pSC-ori Cm^R	*ftsZ-mNeonGreen* (pKECY43 NcoI,XbaI) in pKETS24
pKECY91	*araC* P_{ara} *pdeL*$_{HTH5M}$-*3xFLAG* in pBAD30	*pdeL*$_{HTH5M}$ (PCR T925/OA116, pKECY52) in pKEHB12
pKECY92	*araC* P_{ara} *pdeL*$_{EVL-AAA}$-*3xFLAG* in pBAD30	*pdeL*$_{EVL-AAA}$ (PCR T925/OA116, pKECY53) in pKEHB12
pKECY95	*araC* P_{ara} *rcsB-3xFLAG* (native-RBS) in pBAD30	*rcsB* (PCR T358/S866) in pKEHB12
pKECY96	*araC* P_{ara} *rcsB-3xFLAG* (*T7gene10*-RBS) in pBAD30	*rcsB* (PCR OB93/S866) in pKEHB12
pKECY97	*araC* P_{ara} *rcsB-3xFLAG* (*pdeL*-RBS) in pBAD30	*rcsB* (PCR OB94/S866) in pKEHB12
pKECY98	*araC* P_{ara} *rcsB* (*T7gene10*-RBS) in pBAD30	*rcsB* (PCR OB93/T106) in pBAD30
pKECY99	*araC* P_{ara} *lacI* (*T7gene10*-RBS) in pBAD30	*lacI* (PCR OB155/OB156) in pKECY98
pKECY101	*araC* P_{ara} *rutR* (*T7gene10*-RBS) in pBAD30	*rutR* (PCR OB159/OB160) in pKECY98
pKECY102	*araC* P_{ara} *leuO* (*T7gene10*-RBS) in pBAD30	*leuO* (PCR OA005/T558) in pKECY98
pKECY103	*araC* P_{ara} *cra* (*T7gene10*-RBS) in pBAD30	*cra* (PCR OB161/OB162) in pKECY98

[a] Features include Cm^r (chloramphenicol resistance), Kan^r (kanamycin resistance), MCS (multiple-cloning site), and pSC-rep^{ts} (temperature-sensitive replication, derivative of pSC101).

[b] Cloning was verified by sequencing of the cloned PCR fragments.

401

Figures and Legends

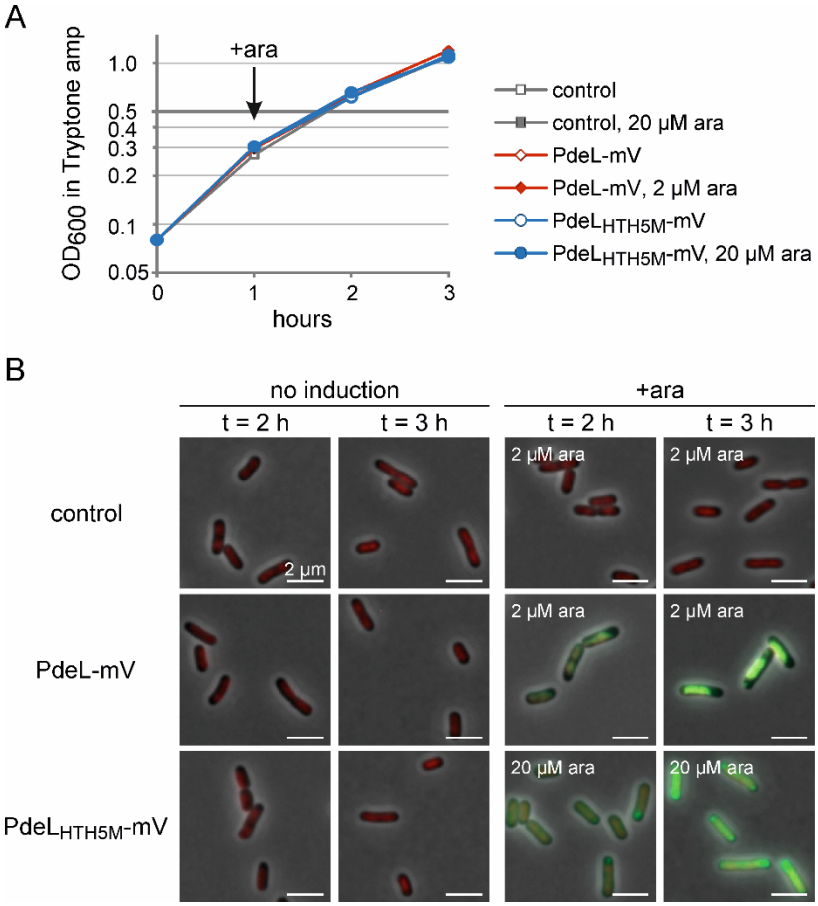

Figure 1 PdeL is nucleoid-associated. (A) Growth of transformants of *hupA-mCherry* Δ*pdeL* strain U159 with plasmids pBAD30 (control), pKECY1 (PdeL-mV) and pKECY11 (PdeL$_{HTH5M}$-mV), respectively. Cultures were inoculated to OD_{600} 0.08 and grown in tryptone ampicillin medium. After one hour of growth (t = 1 h), P_{ara} directed expression was induced with L-arabinose using a final concentration of 2 µM in case of *pdeL-mVenus* and 20 µM in case of *pdeL$_{HTH5M}$-mVenus*. With these inducer concentrations steady state protein levels are similar as tested using 3xFLAG variants of PdeL and PdeL$_{HTH5M}$ (Fig. S1). (B) Composite fluorescent microscopy images of representative bacteria with fluorescence of HupA-mCherry shown in red and of PdeL-mVenus or PdeL$_{HTH5M}$-mVenus (in green). Samples were harvested from un-induced and induced cultures at t = 2 h and t = 3 h. The scale bar corresponds to 2 µm. Full images are shown in supplementary Figure S2.

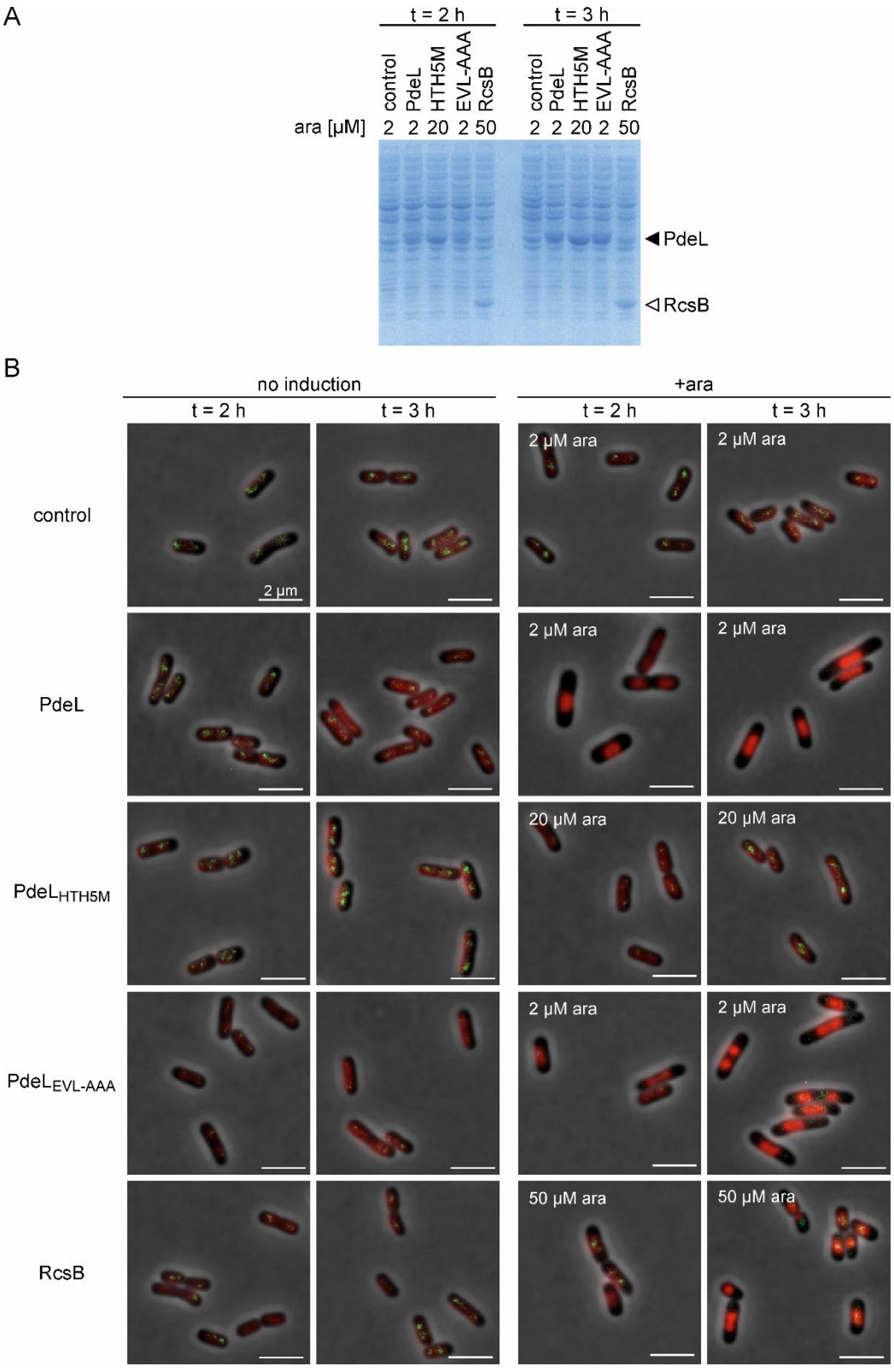

415

416 Figure 2 High levels of PdeL, PdeL$_{EVL-AAA}$ and RcsB cause nucleoid compaction and loss of
417 MukB-mNG foci. Transformants of *hupA-mCherry mukB-mNG* Δ*pdeL* strain U477 with
418 plasmids pBAD30 (control), pKECY44 (PdeL), pKECY52 (PdeL$_{HTH5M}$), pKECY53 (PdeL$_{EVL-AAA}$), and
419 pKECY98 (RcsB), respectively, were grown in tryptone ampicillin medium. After one hour of

growth P_{ara} directed expression of *pdeL* and its mutants as well as of *rcsB* was induced by addition of L-arabinose, as indicated. Samples were harvested after 2 and 3 hours of growth (t = 2h, t= 3h). (A) Protein levels were analyzed by 15% SDS-PAGE and Coomassie staining. Bands corresponding to PdeL proteins and to RcsB are indicated, by filled and open triangles, respectively. (B) Representative sections of microscopy images of transformants expressing no protein (control), PdeL, $PdeL_{HTH5M}$, $PdeL_{EVL\text{-}AAA}$, and RcsB, respectively. HupA-mCherry fluorescence is shown in red and MukB-mNeonGreen foci are shown in green. Full size microscopy images are shown in Fig. S4.

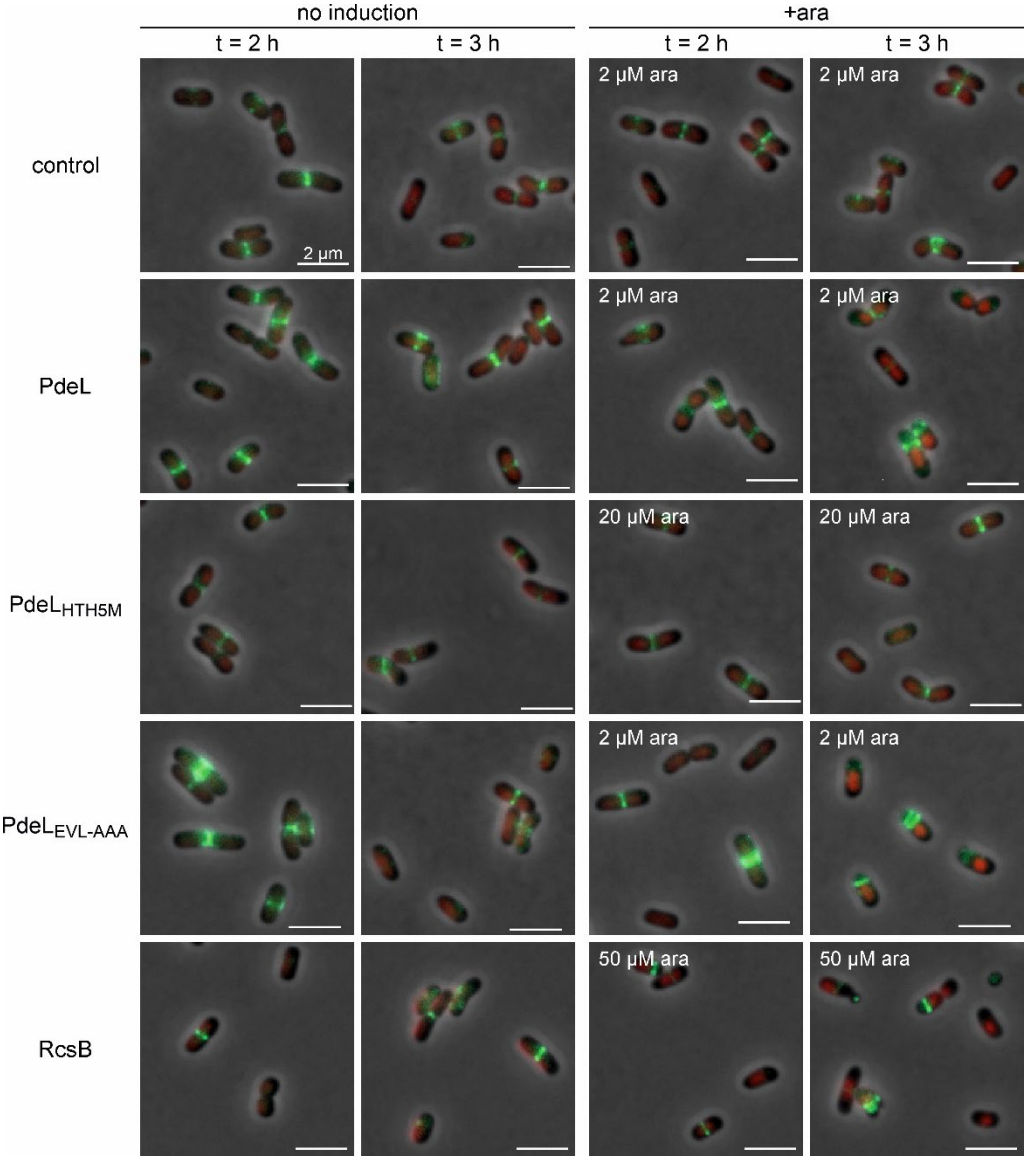

Figure 3: PdeL, PdeL$_{EVL-AAA}$ and RcsB misplace FtsZ rings. For visualization of the Z-ring a C-terminally mNeonGreen tagged FtsZ variant, FtsZ-mNG, was ectopically expressed under the control of P_{lacUV5} promoter using low copy plasmid pKECY90. Co-transformants of *hupA-mCherry* Δ*pdeL* strain U159 with plasmid pKECY90 (P_{lacUV5} *ftsZ-mNG*) and plasmids pBAD30 (control), pKECY44 (PdeL), pKECY52 (PdeL$_{HTH5M}$), pKECY53 (PdeL$_{EVL-AAA}$), and pKECY98 (RcsB), respectively, were grown in tryptone ampicillin chloramphenicol medium. After one hour of growth P_{ara} directed expression was induced by L-arabinose, as indicated. Samples were harvested at t = 2 h and t = 3 h of growth. Shown are representative sections of composite microscopy images of transformants with HupA-mCherry (in red) and FtsZ-mNG (in green). Contrast settings for RcsB images were adjusted for better visibility of FtsZ-mNG to 180-700 (mNG) and 200-2000 (mCherry). Full size images are shown in Fig. S6.

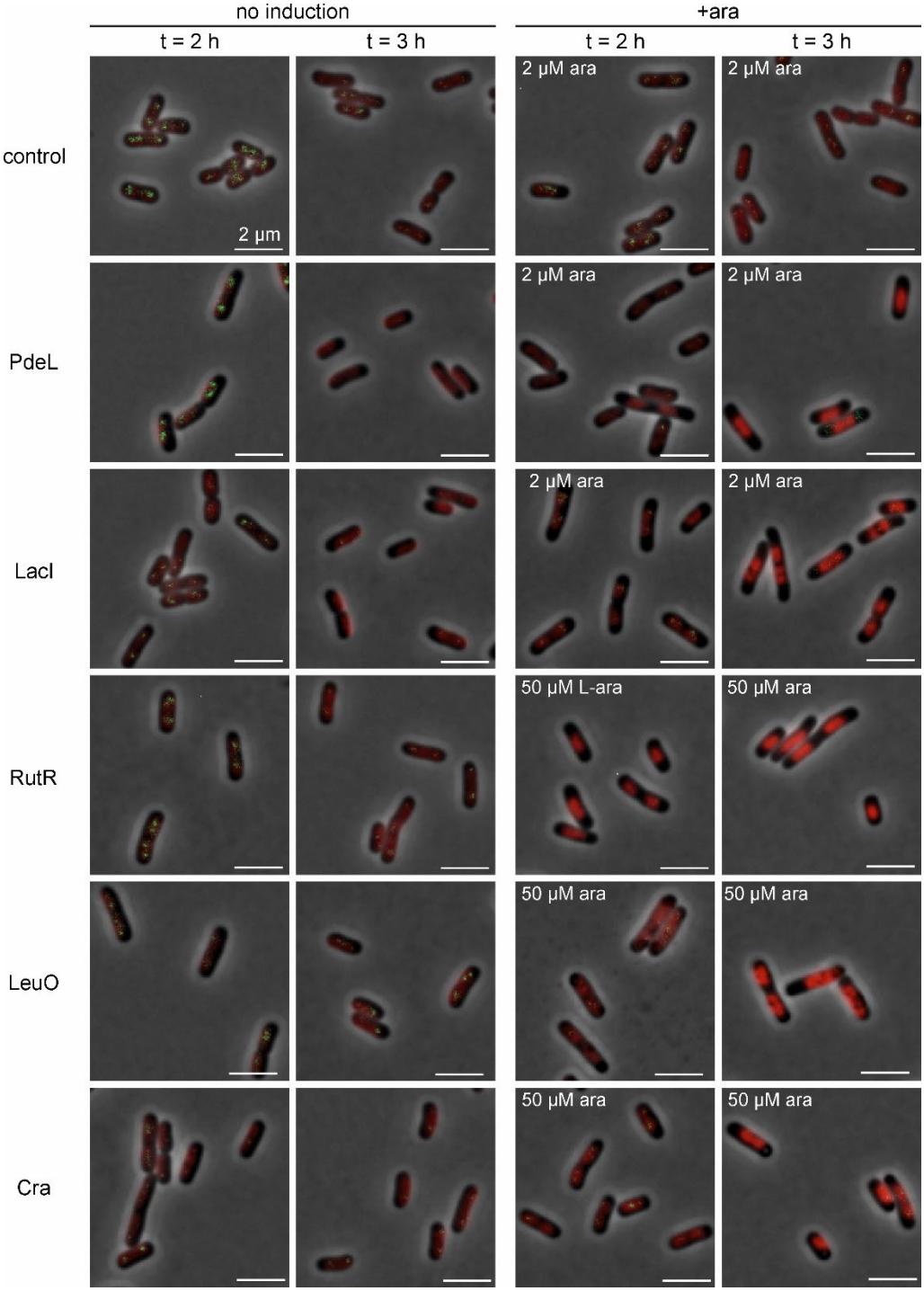

Figure 4: High levels of the transcription regulators LacI, RutR, LeuO, and Cra cause nucleoid compaction and loss of MukB foci. Transformants of *hupA-mCherry mukB-mNG* Δ*pdeL* strain U477 with plasmids pBAD30 (control), pKECY44 (PdeL), pKECY99 (LacI), pKECY101 (RutR), pKECY102 (LeuO), and pKECY103 (Cra) were grown in tryptone ampicillin medium. After one hour of growth, P_{ara} directed expression of transcription regulators was induced with L-arabinose, as indicated. Expression of similar amounts of the transcription regulators was

447 analyzed SDS-PAGE (Fig. S7). Shown are representative composite microscopy images (full
448 size images are shown in Fig. S8).

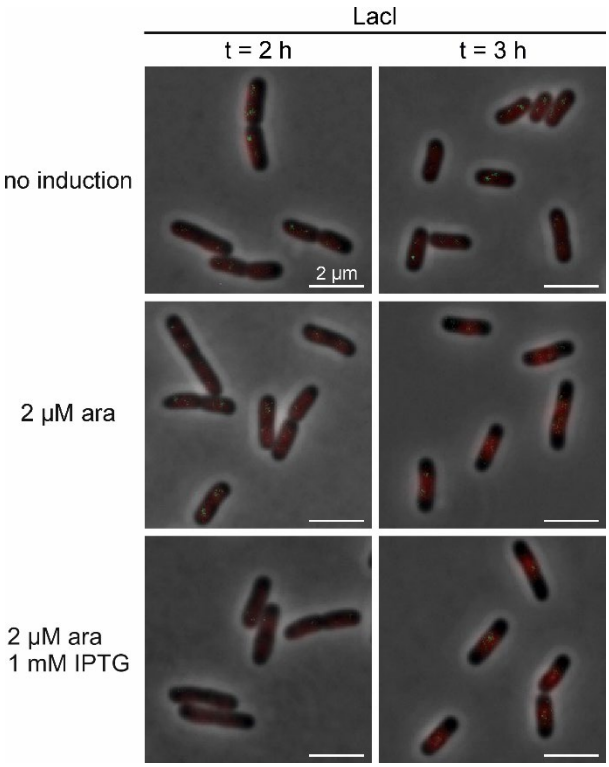

449

450 Figure 5: Non-specific DNA-binding by LacI causes nucleoid compaction. To test whether non-
451 specific DNA-binding by LacI causes nucleoid compaction IPTG was added as well to cultures
452 of transformants of *hupA-mCherry mukB-mNG* Δ*pdeL* strain U477 with plasmid pKECY99
453 (LacI). After one hour of growth in tryptone ampicillin medium *lacI* expression was induced
454 with 2 µM L-arabinose and IPTG was supplemented to a final concentration of 1 mM, where
455 indicated. Samples were harvested after one (t = 2h) and two (t = 3h) hours of growth. Shown
456 are representative composite microcopy images; full size images are shown in Fig. S9.

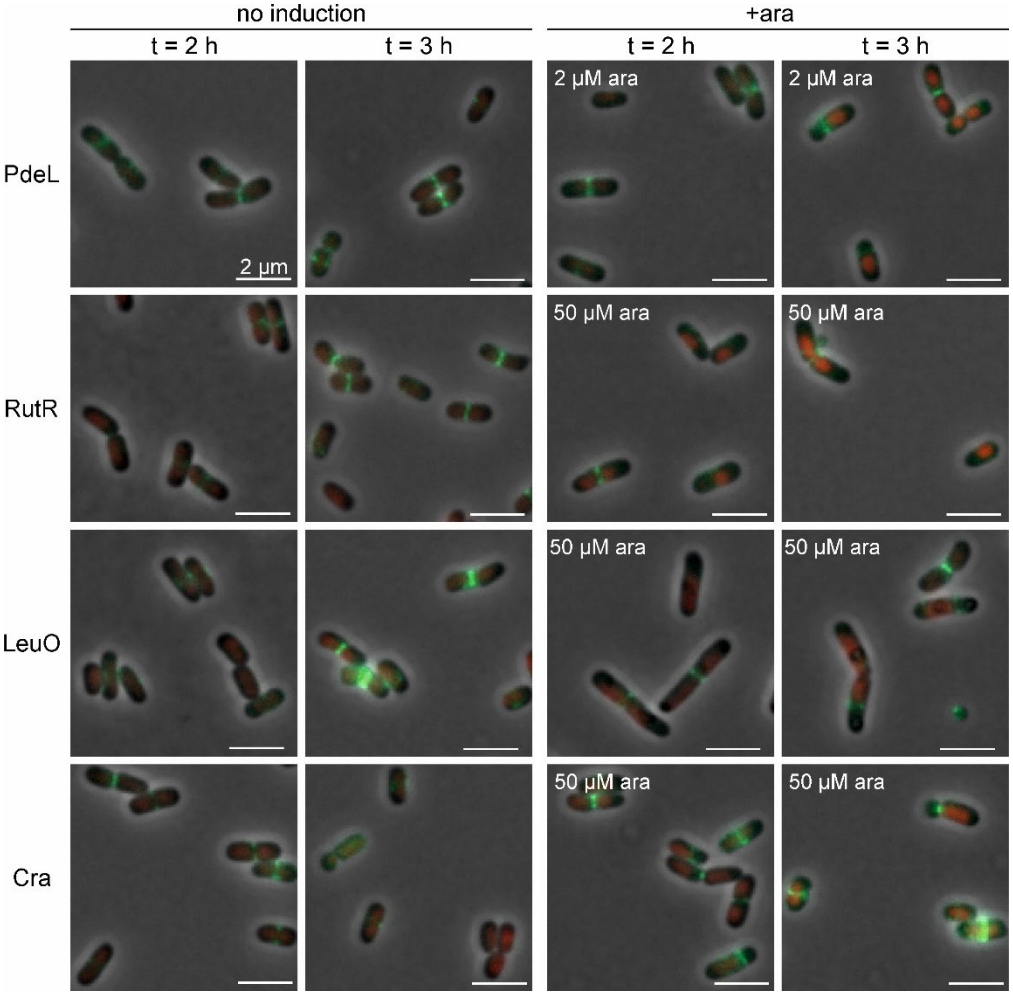

Figure 6: Cell division protein FtsZ is misplaced upon overexpression of transcription regulators RutR, LeuO and Cra. Co-transformants of *hupA-mCherry* Δ*pdeL* strain U159 with plasmids pKECY90 (FtsZ-mNG) and pKECY44 (PdeL), pKECY101 (RutR), pKECY102 (LeuO) and pKECY103 (Cra) were grown in tryptone medium supplemented with chloramphenicol and ampicillin. After one hour of growth P_{ara} directed expression of transcription regulators genes were induced with L-arabinose, as indicated, and samples were harvested after two (t= 2 h) and three (t = 3h) hours of growth. Representative composite microscopy images with FtsZ-mNG (shown in green) and HupA-mCherry (in red). Full size images are shown in Fig. S10.